Available online at www.sciencedirect.com

ScienceDirect

Advances in Space Research xxx (2014) xxx–xxx

ADVANCES IN SPACE RESEARCH (a COSPAR publication)

www.elsevier.com/locate/asr

Adaptive recognition and correction of baseline shifts from collocated GPS and accelerometer using two phases Kalman filter

Rui Tu [a,b,*], Rongjiang Wang [a], Thomas R. Walter [a], FaQi Diao [a,c]

[a] German Research Center for Geosciences (GFZ), Telegrafenberg, 14473 Potsdam, Germany
[b] University of Potsdam, Am Neuen Palais, 14469 Potsdam, Germany
[c] Institute of Geodesy and Geophysics, Chinese Academy of Sciences, 430077 Wuhan, China

Received 4 April 2014; received in revised form 2 July 2014; accepted 6 July 2014

Abstract

The real-time recognition and precise correction of baseline shifts in strong-motion records is a critical issue for GPS and accelerometer combined processing. This paper proposes a method to adaptively recognize and correct baseline shifts in strong-motion records by utilizing GPS measurements using two phases Kalman filter. By defining four kinds of learning statistics and criteria, the time series of estimated baseline shifts can be divided into four time intervals: initialization, static, transient and permanent. During the time interval in which the transient baseline shift is recognized, the dynamic noise of the Kalman filter system and the length of the baseline shifts estimation window are adaptively adjusted to yield a robust integration solution. The validations from an experimental and real datasets show that acceleration baseline shifts can be precisely recognized and corrected, thus, the combined system adaptively adjusted the estimation strategy to get a more robust solution.

Keywords: GPS; Strong-motion; Baseline shift; Kalman filter; Integration

1. Introduction

Digital accelerographs, with advantages of low-cost and high sample rate (80–200 Hz), typically are used to record strong ground motions and are commonly used for earthquake monitoring and early warning (Graizer, 1979; Chiu 1997; Zhu 2003). However, these instruments can only provide high-precision acceleration waves; velocity and displacement waves are obtained from the acceleration by integration (Elósegui et al., 2006; Genrich and Bock, 2006; Larson et al., 2007). Tilting and/or rotation of the ground that may occur during the co-seismic period and instrumental effect can introduce baseline shifts (small steps or distortions in the reference level of the acceleration), which prevent recovery of true ground velocities and displacement through double integration. On the contrary, the GPS measurements can get high precision displacement information, but the velocity and acceleration information usually involve large uncertainties caused by environmental and instrument noised (Elósegui et al., 2006), meanwhile, the GPS sample rate is also very low (a few Hz).

Currently, different empirical methods are used to approximately correct for the baseline shifts (Iwan et al., 1985; Boore 2001; Zhu 2003; Graizer 2006; Wu and Wu 2007; Wang et al., 2011). As the baseline shift can happen at any time and change temporally, especially during the co-seismic period, these empirical methods generally cannot accurately recognize and correct these transient baseline

* Corresponding author at: The German Research Centre for Geosciences (GFZ), Kaiser Friedrich Str. 142, 14469 Potsdam, Germany. Tel.: +49 331 288 28821; fax: +49 331 288 1204.
E-mail addresses: turui-2004@126.com (R. Tu), wang@gfz-potsdam.de (R. Wang), twalter@gfz-potsdam.de (T.R. Walter), diao@gfz-potsdam.de (F. Diao).

http://dx.doi.org/10.1016/j.asr.2014.07.008
0273-1177/

shifts, and the derived results usually display large offsets when compared to geodetic survey results, i.e., Wang et al. (2013) point out the RMS of the deviatoric displacement vectors between the GPS and strong-motion data is 0.47 m for the 2011 Mw 9.0 Tohoku-Oki earthquake.

Rightnow, several methods are being developed to utilize high precision GPS to correct for baseline shifts in strong-motion records. These methods can be divided into two categories. The first is loose integration, which uses high-precision GPS displacement as constrain to get precisely solutions. In Bock et al. (2011), the baseline shifts are absorbed by the dynamic noise of a Kalman filter. In Wang et al. (2013), the baseline shifts are expressed by a trigonometric function polynomial, and a least-squares solution was used to determine the baseline shifts by making the corrected displacements optimally consistent with the high-rate GPS displacement. In Tu et al. (2013), the baseline shifts are directly obtained from the difference between the GPS displacements and acceleration-integrated displacements. In Huang et al. (2013), they used the GPS results as constrains to select the suitable corner frequency for the empirical mode decomposition (EMD) derived baseline correction scheme. The second category is tight integration, which directly uses GPS raw data calculating baseline shift for strong-motion records. In Geng et al. (2013a), the baseline shifts are modeled as a random walk process to be estimated together with displacements. In Tu et al. (2014) the baseline shifts are estimated firstly by Precise Point Positioning (PPP), then applied to the motions derived from acceleration to recover the coseismic waves. Moreover, while considering the baseline shifts are caused by the ground tilts (Graizer 2005, 2006), the coseismic point ground tilts can be recovered from collocated high-rate GPS and accelerometers (Geng et al., 2013b). In cases where there are no baseline shifts or baseline shifts are robustly corrected, the high resolution acceleration records can be used to strengthen GPS for a better solution.

Overall, the precise recognition and correction of baseline shifts in strong-motion records is important to get the robust and broadband ground motion information for GPS and strong-motions combined system. In this study, we present an improved tight integration of baseline correction method based on two phases Kalman filter. Compare to the previous one phase Kalman filter integration approach (such as Geng et al., 2013a and Tu et al., 2014), the two phases Kalman filter approach is an adaptive filter procedure, it constructs a suitable learning static to detect the disturbanced state and adaptively adjusts the estimation strategy. By defining four kinds of learning statistics and criteria, we analyze the time series of estimated baseline shifts from the first phase Kalman filter and determine the state of the baseline shift, then adaptively adjust the dynamic noise of the combined system and the length of the baseline shift estimation window for the second phase Kalman filter to yield a robust integration solution. The validations from an experimental and real datasets shown that acceleration baseline shifts can be adaptively recognized and precisely corrected, the recovered ground motion information from two phase Kalman filter approach are more reliable than one phase Kalman filter approach after adaptive adjusting the estimation strategy. After an overview of the integration model that utilizes both GPS and strong-motion records, the baseline shift adaptive-recognition theory is introduced, then an experimental and real dataset is used for validation, and finally some conclusions are made.

2. Methodology

2.1. The model for tight integration of GPS and strong-motion measurements

Usually the following observation equations are used for the tight integration of GPS and strong-motion measurements (Tu et al., 2014; Geng et al., 2013a).

$$\begin{bmatrix} L_c \\ P_c \end{bmatrix}_k = \begin{bmatrix} e_k & m_{z,k} & 1 & 1 \\ e_k & m_{z,k} & 1 & 0 \end{bmatrix} \begin{bmatrix} \mathrm{x}_k \\ z_k \\ \delta t_k \\ b \end{bmatrix} + \begin{bmatrix} \varepsilon_{L_c} \\ \varepsilon_{P_c} \end{bmatrix}, \quad \begin{matrix} \varepsilon_{L_c} \sim N(0, \sigma^2_{L_c}) \\ \varepsilon_{P_c} \sim N(0, \sigma^2_{P_c}) \end{matrix} \tag{1}$$

$$a_k = \ddot{\mathrm{X}}_k + u_k + w_{a_k}, \quad w_{ak} \sim N(0, \sigma^2_{W_{ak}}) \tag{2}$$

where, L_c and P_c are the observed minus computed phase and pseudorange observations from satellite to receiver, respectively, e is the unit direction vector from satellite to receiver, m is the tropospheric mapping function for wet delay, x and $\ddot{\mathrm{X}}$ denote the vectors of the receiver displacement and acceleration, z, δt and b are the tropospheric zenith delay, receiver clock and phase ambiguities, ε is the measurement noise, with variances σ^2, W_{ak} is the acceleration observation noise, a and u represent the strong-motion acceleration observation and baseline shift, and k is the epoch number. The baseline shift is estimated as a constant in each estimation window. The other parameters, like the zenith tropospheric delay, can be estimated as a constant over a short time-span (one hour or two hour) or represented by a random-walk process, while receiver clock bias is estimated epoch-by-epoch and the ambiguity is estimated as a constant (Kouba and Héroux, 2001; Dach et al., 2007).

The state equations for the station movement and baseline shifts are expressed as follows.

$$\begin{bmatrix} \mathrm{X}_k \\ \dot{\mathrm{X}}_k \\ \ddot{\mathrm{X}}_k \\ u_k \end{bmatrix} = \begin{bmatrix} \mathbf{I} & 0.5\mathbf{I}\tau & 0.5\mathbf{I}\tau^2 & 0 \\ 0 & \mathbf{I} & \mathbf{I}\tau & 0 \\ 0 & 0 & \mathbf{I} & 0 \\ 0 & 0 & 0 & \mathbf{I} \end{bmatrix} \begin{bmatrix} \mathrm{X}_{k-1} \\ \dot{\mathrm{X}}_{k-1} \\ a_k - \hat{u}_{k-1} \\ u_{k-1} \end{bmatrix} + W_k, \tag{3}$$

where $\dot{x}$ is the velocity vector, $\mathbf{I}$ is a 3×3 identity matrix, τ is the smallest sampling rate of the integrated sensors. w_k is the dynamic noise, with the expectation $E(w_k) = 0$ and

Please cite this article in press as: Tu, R., et al. Adaptive recognition and correction of baseline shifts from collocated GPS and accelerometer using two phases Kalman filter. J. Adv. Space Res. (2014), http://dx.doi.org/10.1016/j.asr.2014.07.008

variance $D(W_k) = \begin{bmatrix} \frac{\tau^4}{20}q_u^2\mathbf{I} & \frac{\tau^3}{8}q_u^2\mathbf{I} & \frac{\tau^2}{6}q_u^2\mathbf{I} & 0 \\ \frac{\tau^3}{8}q_u^2\mathbf{I} & \frac{\tau^2}{3}q_u^2\mathbf{I} & \frac{\tau^1}{2}q_u^2\mathbf{I}0 & \\ \frac{\tau^2}{6}q_u^2\mathbf{I} & \frac{\tau^1}{2}q_u^2\mathbf{I} & q_u^2\mathbf{I} & 0 \\ 0 & 0 & 0 & q_u^2\mathbf{I} \end{bmatrix}$ respectively, q_u is the power density of the baseline shift. Here, the baseline-shift-corrected acceleration $(a_k - \hat{u}_{k-1})$ was used instead of the predicted acceleration $(a_{k\text{-}1})$ to avoid both the acceleration and the baseline shift having large dynamic noise, so only dynamic noise of the baseline shift needs to be determined optimally (Tu et al., 2013).

With equations (1), (2) and (3), a Kalman filter can be employed for the parameters estimation while given an empirical observation weight and dynamic noise (Hauschild and Montenbruck, 2009; Tu et al., 2014). Moreover, the stochastic model can be adaptively adjusted for a more robust estimation (Jin et al., 2005, 2010).

2.2. The adaptive recognition of baseline shifts in strong-motion records

For the robust integration of GPS and strong-motion records, we need to solve two critical problems. The first one is whether a baseline shift has happened. If so, then we can estimate the duration of the baseline shift. The second is to determine how significant a baseline shift is. Then, we can determine the optimal dynamic noise for the state vector.

To tackle these problems, an adaptive filter procedure can be used. Some learning statistics need to be defined in order to detect whether a baseline shift has happened, to identify how significant it is, and then make an adaptive estimation of the shift. In the literature, learning statistics for navigation are usually defined based on state discrepancy, variance component and predicted residuals, from which adaptive solutions are obtained (Yang et al., 2001; Yang and Gao, 2006; Wang et al., 2000; Hu et al., 2003). But they cannot well be used for the GPS and strong-motion integrated system. On one side, for the GPS and strong-motion integration system, which introduces the baseline shifts and phase ambiguity parameters, the geometric state may be badly estimated or even cannot be estimated by the limited observations of a single epoch. In this case the statistical characteristics of the state discrepancy or variance component will be poor. On the other side, the baseline shifts in strong-motion records are very sensitive when integrated into velocity and displacement. Although the values of baseline shifts typically are very small compared to PGA values, they will lead to a significant effect on the integrated displacements (Boore, 2001; Boore et al., 2002; Wang et al., 2011). Moreover, the baseline shifts are mainly caused by the tilting and/or rotation of the ground, and have an important feature that it is zero or a constant value while there is no motion (Iwan et al., 1985; Graizer 2006; Wang et al., 2011; Geng et al., 2013b), so it is more sensitive to select the baseline shifts as learning statistics. Meanwhile, the high resolution acceleration signal can also be used to detect the state motions. With the assumption that the baseline shifts and acceleration are zero during static states, then we defined four learning statistics to recognize whether there exist baseline shifts and how significant they are. As the strong-motion has a much higher sample rate than the GPS, the length of the baseline shift estimation window is selected as the duration of the GPS sample interval. Meanwhile, the baseline shifts and accelerations are integrated into displacement in the whole baseline shift estimation window to avoid the influence of random error.

$$\text{learning statistic one}: A = \iint_{t_1}^{t_2} (u - 0) \cdot dt \quad \begin{matrix} A_1 : (A < A_0) \\ A_2 : (A \geqslant A_0) \end{matrix}, \tag{4}$$

$$\text{learning statistic two}: B = \iint_{t_1}^{t_2} (a - 0) \cdot dt \quad \begin{matrix} B_1 : (B < B_0) \\ B_2 : (B \geqslant B_0) \end{matrix}, \tag{5}$$

$$\text{learning statistic three}: C = \iint_{t_1}^{t_2} (\ddot{x} - 0) \cdot dt \quad \begin{matrix} C_1 : (C < C_0) \\ C_2 : (C \geqslant C_0) \end{matrix}, \tag{6}$$

$$\text{learning statistic four}: D = \sqrt{\sum_{i=n_{t_1}}^{n_{t_2}} (a_i - \bar{a})^2 / (n_{t_2} - n_{t_1})} \quad \begin{matrix} D_1 : (D < D_0) \\ D_2 : (A \geqslant D_0) \end{matrix}, \tag{7}$$

where, t_1, t_2 define the estimation time window; n_{t1}, n_{t2}, is the epoch number, $\bar{a}$ is the mean value of a, A represents the displacement effect of the solved baseline shifts, B represents the displacement effect of the raw acceleration, C represents the displacement effect of the corrected acceleration, and D represents the signal strength. Each of the four learning statistic has two cases that depend on the defined criteria of A_0, B_0, C_0 and D_0. The criteria were calculated by three times of the standard deviation from the time series of each learning statistic during the static period.

Based on the defined learning statistic and criteria, the estimated baseline shifts can be analyzed and adaptively recognized. They can be divided into four time intervals, as shown in Fig. 1. Here, the data come from a shaking table test, it is one of the experiments in Tu et al. (2014), which is described in Section 3.1.

Initialization period: $(A_2\&B_1)$ or $(B_1\&C_2)$, 0–47 s in Fig. 1b. The beginning of the data solution. There is no motion and the raw acceleration is nearly zero (see Fig. 1a, here in order to show the noise of the acceleration record, the amplitude of the vertical axis is limited to 0.2 m/s^2), but the solved baseline shift is not zero (see Fig. 1b). However, the solved baseline shift needs time to converge to finish the initialization. The dynamic noise of the baseline shift should have a very small value.

Static period: (A_1), 47–95 s in Fig. 1b. In this period, the solved baseline shift is nearly zero and the dynamic noise of the baseline shift also should be very small.

Please cite this article in press as: Tu, R., et al. Adaptive recognition and correction of baseline shifts from collocated GPS and accelerometer using two phases Kalman filter. J. Adv. Space Res. (2014), http://dx.doi.org/10.1016/j.asr.2014.07.008

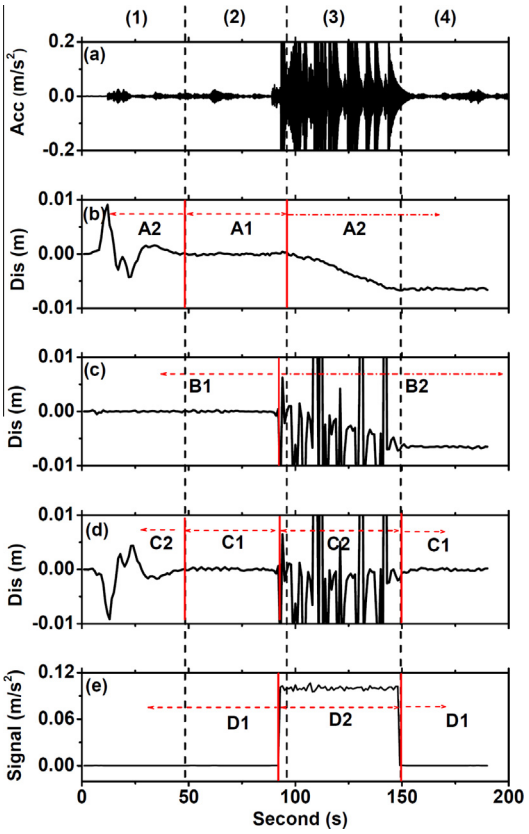

Fig. 1. Adaptive recognition of baseline shifts. Panels (a) represents the raw acceleration observation, (b)–(e) represent four kinds of learning statistics (A, B, C and D in equations (4)–(7)), and (1), (2), (3) and (4) are four periods of the estimated baseline shifts (see text).

Transient baseline shift period: (A_2&D_2), 95–150 s in Fig. 1b. In this period, the baseline shift is detected, and there is a significant signal; the dynamic noise of the baseline shift should be adjusted with a much larger value.

Permanent baseline shift period: (A_2&D_1) & (B_2 & C_1), 150 s to the end in Fig. 1b. In this period, the baseline shift is also detected, but there is no significant signal, the dynamic noise of the baseline shift should be a much smaller value.

During the time interval in which the transient baseline shift is detected, the dynamic noise is adjusted as follows,

$$q'_u = \sqrt{\frac{|u_{t_2} - u_{t_1}|}{(t_2 - t_1)}} \tag{8}$$

where, q'_u is the new power density of the baseline shift, which reflects the actual temporal change of the acceleration baseline shifts. In additional, the length of the estimated baseline shift window can be adaptively adjusted according to the signals: if there is no signal, such as case D_1, the baseline shifts are mainly caused by the environment variation and will be changed very slowly, so we can estimate the baseline shifts at intervals of several seconds or longer, it is an average value of the time window, we used five seconds in this study; otherwise, such as case

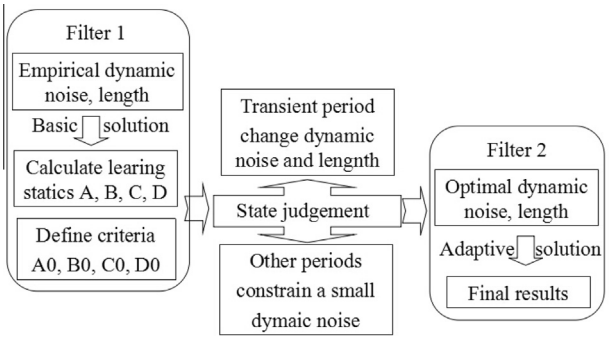

Fig. 2. The flowchart of the data solution. Filter 1 and filter 2 are employed for the basic solution and adaptive solution.

D_2, the baseline shifts are mainly caused by the tilting and/or rotation of the ground motion and will be changed very swift, so it should be estimated at intervals of one second or less to discover the variation of the baseline shift and adjust the dynamic noise, we used one second.

It should be recognized that if a transient baseline shift and state motion exist at the beginning of the data solution, our method cannot work, as it needs a period of static record (about one minute) to initialize.

2.3. The implementation process

The adaptive recognition and correction of baseline shifts outlined in Fig. 2. Two Kalman filters are employed for the combination solution. Filter 1 is used for the basic solution to judge the motion state and determine the optimal dynamic noise and the length of the baseline shift estimation window, and filter 2 is used for the adaptive solution to get the robust integration results. By the empirical weight and dynamic noise (Here, the empirical weight is determined by the measurement noise, such as $\sigma_{P_c} = 0.3$ m, $\sigma_{L_c} = 0.003$ m and $\sigma_{w_a k} = 0.03$ m, dynamic noise is given as a constant, such as $q_u = 0.003\ \mathrm{m}^{1/2}/\mathrm{s}^{3/2}$, the window length is five seconds), we firstly applied the first filter to estimate the baseline shifts, then the time series and criteria for the four kinds of learning statistics are

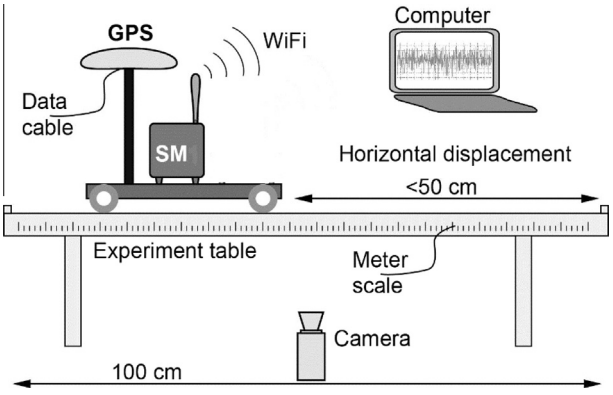

Fig. 3. The experimental platform, including a GPS receiver, a strong-motion sensor (SM) and a video camera.

Please cite this article in press as: Tu, R., et al. Adaptive recognition and correction of baseline shifts from collocated GPS and accelerometer using two phases Kalman filter. J. Adv. Space Res. (2014), http://dx.doi.org/10.1016/j.asr.2014.07.008

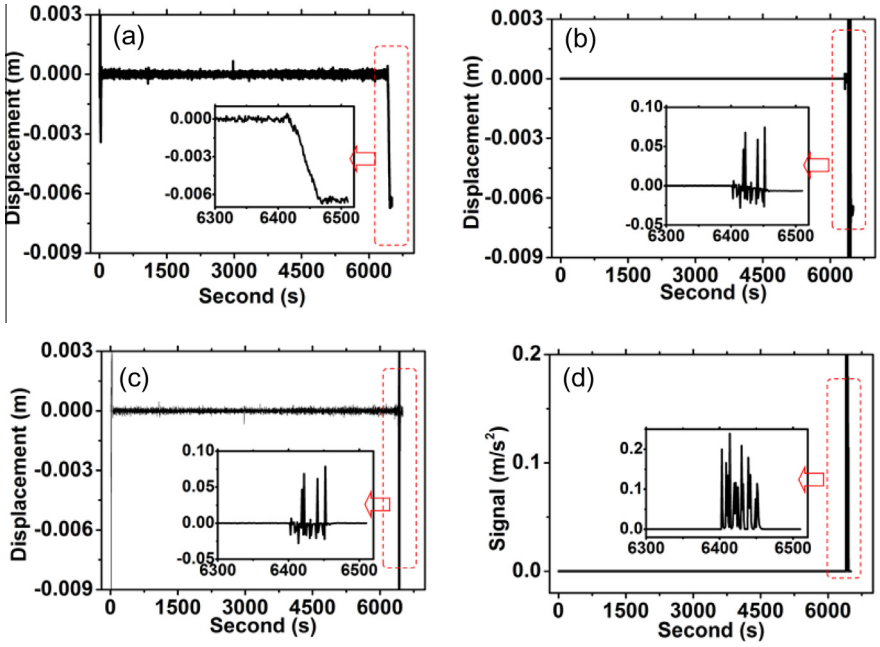

Fig. 4. The determination of the baseline shift parameters. (a)–(d) represent time series of estimated learning statistics A, B, C and D respectively.

calculated and defined. Thus, from the analysis of these, the motion state can be justified. While it is a transient baseline shift period, the dynamic noise is changed according to the variation of the transient baseline shift, the length of the baseline shift estimation window is changed to one second. For the other state periods, the dynamic noise is constrained to a small value (such as $q_u = 0.0001\ m^{1/2}/s^{3/2}$), and the window length is kept with five seconds. Then, employ the second filter for the adaptive solution to get the final results.

3. Validation

The two phases Kalman filter-based baseline correction method is validated by two different datasets: (1) an experimental dataset with the GPS and accelerometer observations simultaneously collected on a dedicated shaking table, and (2) the GPS and accelerometer data collected from the 2011 Mw 9.0 Tohoku earthquake. We used two different solution approaches for comparison. The one phase Kalman filter approach used the empirical dynamic noise and estimated the baseline shift parameters every epoch (named as "Old" based on Tu et al., 2014). The two phases Kalman filter approach adaptively adjust the dynamic noise and the length of the baseline shifts estimation window based on the one phase Kalman filter results (named as "New").

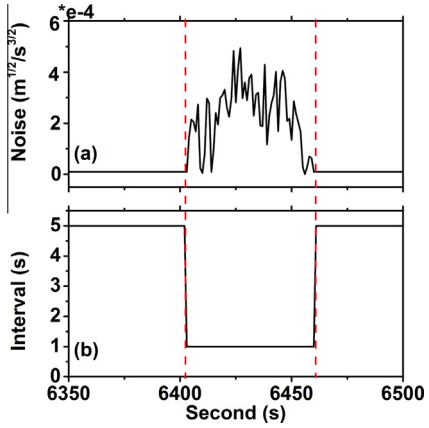

Fig. 5. The analysis of the dynamic noise (a) and length of baseline shift estimation window (b). Note the difference in the window duration as compared to Fig. 4.

3.1. Experimental test using a shaking table

The experimental platform is shown schematically in Fig. 3. The GPS antenna and strong-motion sensor can slide along the rail, a camera system (50 Hz) was also set up to record the sledge motion from a distance of 10 m (Walter 2011). The 1 Hz GPS and 100 Hz strong-motion records were used for the data analysis. Baseline shifts of the strong-motion record were caused mainly by the shifting weight of the cart as it moves along the track. After acquiring a long static record, a simple and one-dimensional movement was introduced by sliding the sensors along the track forwards in step-wise with various accelerations, it last about one minute and with max acceleration 1.5 m/s^2, finally resulting in a permanent displacement of 0.3 m.

Fig. 4 shows the process of the baseline shift recognition. After 52 s of initialization the baseline shift estimation solution converges. From 52 to 6405 s is a zero baseline shift period. At second 6405 the transient baseline shift is

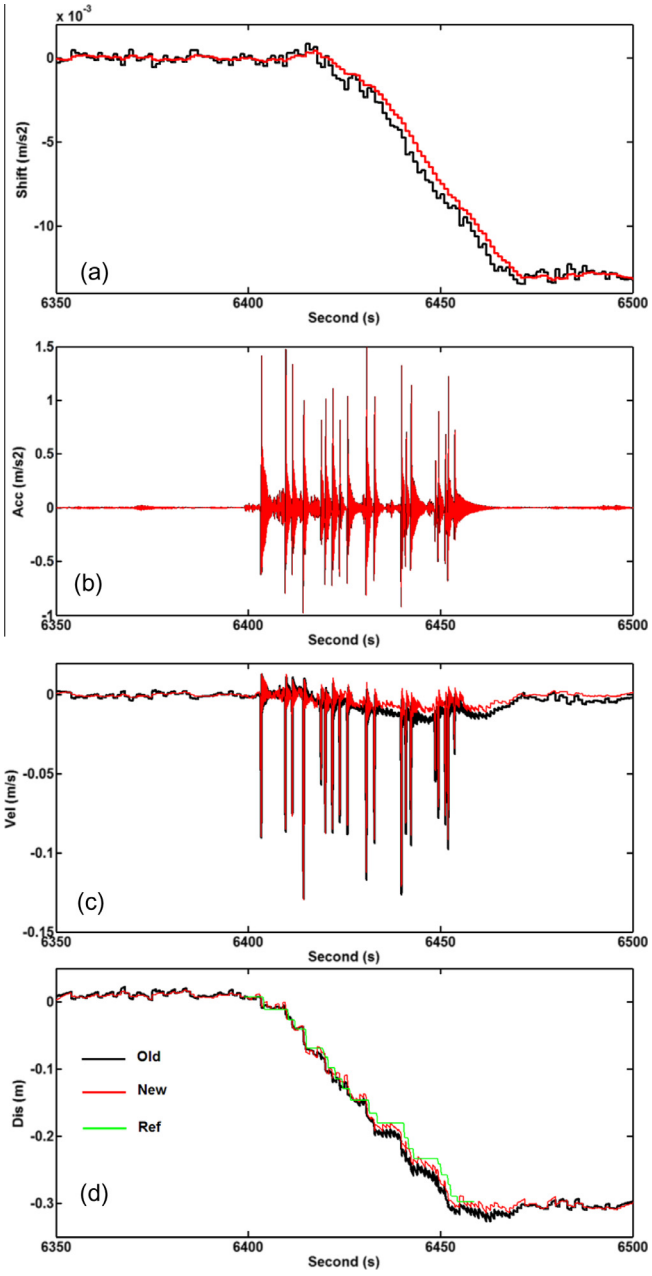

Fig. 6. The time series of the combined results, the black line marks the basic results from one phase Kalman filter (Old), the red line marks the adaptive results from two phases Kalman filter (New), the green line marks the reference displacement from the camera images (Ref). (a)–(d) represent the baseline shift, acceleration, velocity and displacement respectively.

detected and lasts until second 6460. From 6460 s to the end is the permanent baseline shift period. The A_0, B_0, C_0 and D_0 were defined by three times of the standard deviation from the time series of each learning statistic during the static period. The values of A_0, B_0, C_0 and D_0 are $2.9e^{-4}$, $4.0e^{-5}$, $3.2e^{-4}$ m and $1.5e^{-2}$ m/s^2, respectively, in this study.

Fig. 5a shows the dynamic noise of the baseline shifts. It can be clearly seen that in the motion period, when the transient baseline shifts, the dynamic noise was adaptively

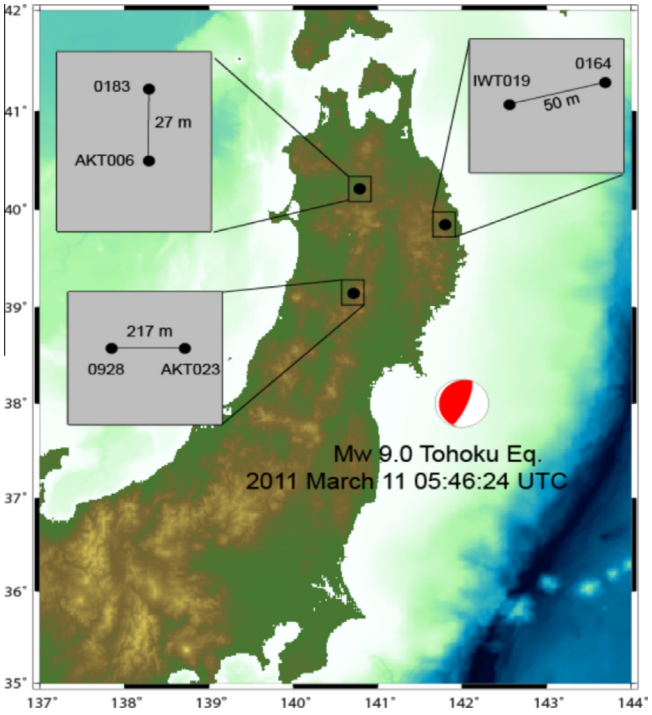

Fig. 7. The Japan Tohoku earthquake (Mw 9.0), occurred on 2011 March 11 05:46:24 UTC at 38.297°N, 142.372°E. The big round shows the epicenter location, the co-located GPS and seismic pairs are (0183-AKT006), (0164-IWT019) and (0928-AKT023).

adjusted to a large value. Conversely, during the rest time, there is very small dynamic noise (we use 0.00001 m$^{1/2}$/s$^{3/2}$). The small dynamic noise and high resolution acceleration would be helpful to strengthen GPS solutions for fast convergence of integer ambiguity and consequently better accuracy. Fig. 5b shows the length of the baseline shift estimation window. During times of rest there is no signal and no transient baseline shift, the length of the baseline shift estimation window can be very large. When there is motion, the length of the baseline shift estimation window should be decreased. In this study, the baseline shift is estimated every five seconds at rest time and one second during times of motion.

Fig. 6 shows the time series of the baseline shifts, acceleration, velocity and displacement for the adaptive and basic approaches. For the basic approach, the dynamic noise is set as a constant (0.003 m$^{1/2}$/s$^{3/2}$). In Fig. 6a, the difference of the estimated baseline shift between the adaptive method and the basic method is obvious during the motion period. As the magnitude of solved baseline shift is much small compare with the acceleration, we cannot find large difference for the acceleration as shown in Fig. 6b. But this small difference of the solved baseline shifts leads to the estimated displacement with a large high-frequency noise for the basic approach as shown in Fig. 6d. Moreover, from Fig. 6c, the velocity of the basic method with a small bias to zero value when the ground motion is stop, it is inconsistent with the actual, but the adaptive method is OK. In all, the adaptive results are more stable and with a smaller noise than the basic results.

Please cite this article in press as: Tu, R., et al. Adaptive recognition and correction of baseline shifts from collocated GPS and accelerometer using two phases Kalman filter. J. Adv. Space Res. (2014), http://dx.doi.org/10.1016/j.asr.2014.07.008

Table 1
Information of the selected co-located GPS and seismic stations.

GPS	Latitude (°)	Longitude (°)	Seismic	Latitude (°)	Longitude (°)	Distance (m)
0183	40.2154 N	140.7873 E	AKT006	40.2152 N	140.7873 E	27
0164	39.8492 N	141.8039 E	IWT019	39.8491 N	141.8034 E	50
0928	39.1462 N	141.7151 E	AKT023	39.1462 N	141.7170 E	215

3.2. Application to a real earthquake: 2011 Mw 9.0 Tohoku earthquake

To better assess the capability of the improved approach, co-located GPS and strong-motion data collected during the Tohoku earthquake (Mw 9.0, 2011, March 11, 05:46:24 UTC) was also analyzed for obtaining three-dimensional co-seismic waves (Fig. 7). Three pairs of co-located GPS and strong-motion sensor were selected and processed, the station information are shown in Table 1. The GPS data were provided by the Geospatial Information Authority (GSI). And the seismic data collocated by K-Net which is operated by the National Research Institute for Earth Science and Disaster Prevention (NIED). The sample rates are 100 Hz and 1 Hz for the accelerometer and GPS respectively.

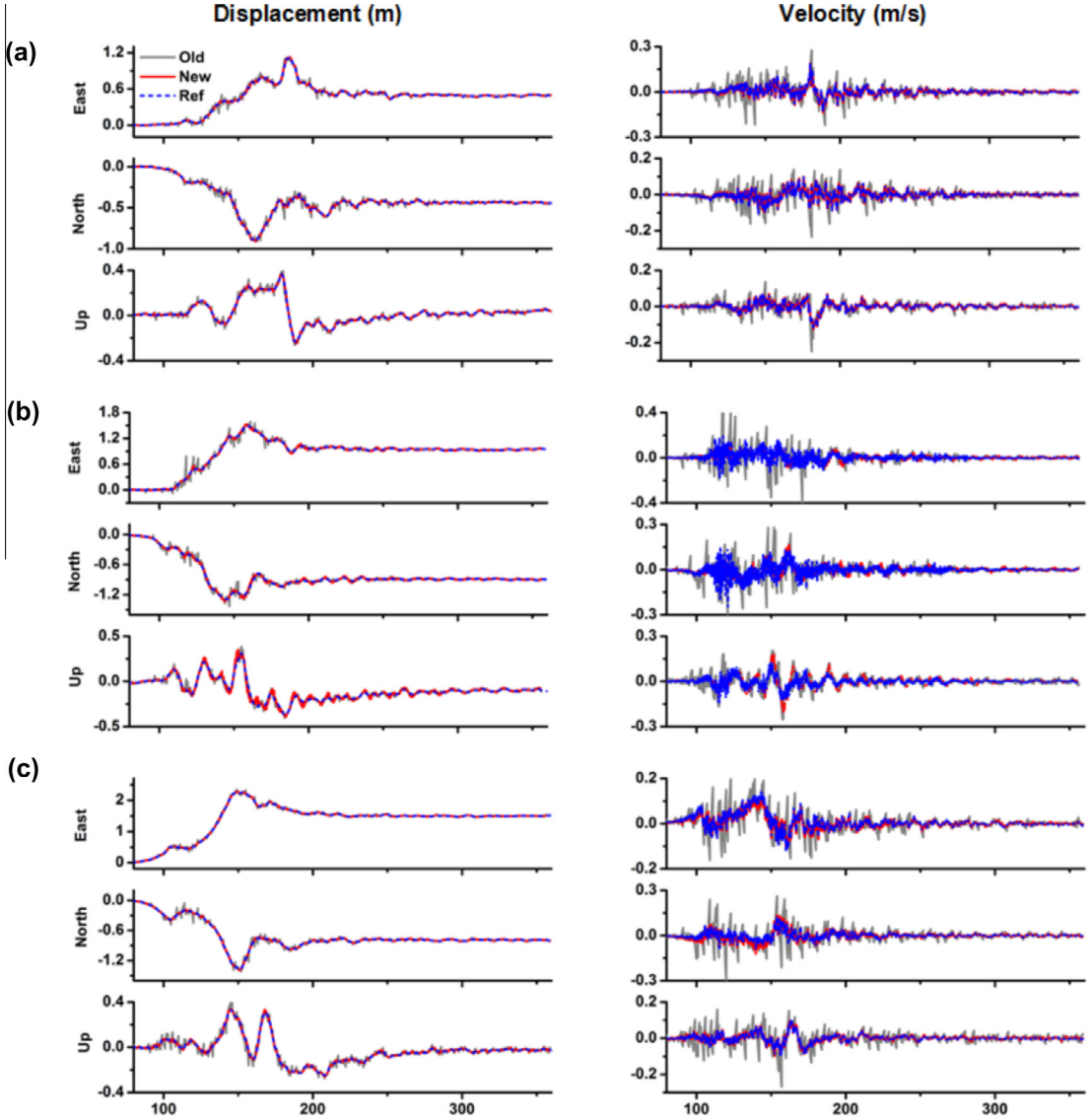

Fig. 8. Results of the co-located GPS and seismic pairs from the 2011 Tohoku earthquake. The left column shows the displacement and the right column shows the velocity. The gray, red and blue color are represent the one phase Kalman filter results ("Old"), the two phases Kalman filter results ("New") and reference results ("Ref") respectively. Here (a), (b) and (c) are for the pair of (0183-AKT006), (0164-IWT019) and (0928-AKT023). The three rows from top to bottom represent East, North and Up component, respectively.

Please cite this article in press as: Tu, R., et al. Adaptive recognition and correction of baseline shifts from collocated GPS and accelerometer using two phases Kalman filter. J. Adv. Space Res. (2014), http://dx.doi.org/10.1016/j.asr.2014.07.008

The results are shown in Fig. 8. The estimated displacements are plotted on the left column, and the velocities are plotted on the right column. The one phase Kalman filter results ("Old"), the two phases Kalman filter results ("New") and reference results ("Ref") are in gray, red and blue color respectively. Here, the reference displacement is calculated by PPP post-processing solutions, the reference velocity is calculated by the empirical baseline correction approach of Wang et al. (2011). It can be clear seen that the new results is best consistent with the reference results, and the old results with large noises and biases, especially during the strong motion period. The reason is that, the change of baseline shifts are very swift during the strong motion period, one phase Kalman filter used the empirical dynamic noise cannot best fit the motion state that lead to the state equations estimation with a divergency, so there are some biases compare to the reference values. As the GPS sample rate is lower than the seismic sensor sample rate, during the interval of two adjacent GPS epochs, we just performing the Kalman filter prediction and applying the filter update stage only when a GPS sample becomes available, so the divergency of the state equations estimation will lead the results with high frequency spike during two adjacent GPS epochs. As the displacement parameters are also constrained by the high precision GPS observation equation, and the velocity parameters are only controlled by the state equations, so the high frequency spike is more serious in velocity. But for the two phases Kalman filter, it adaptively adjust the dynamic noise and best fit the motion state, so we get a much better solutions.

4. Conclusion

This paper proposes an improved tight integration of baseline correction method from collocated GPS and accelerometer. The tight integration model and two phases Kalman filter are used for the combined data solution. By the defined four learning statistic and criteria, the time series of estimated baseline shifts can be divided into four intervals: initialization, static, transient baseline shift, and permanent baseline shift. Once the transient baseline shift is recognized, the dynamic noise and the length of the baseline shift estimation window are adaptively adjusted for a robust integration solution. The validations show that, the acceleration baseline shifts can be adaptively recognized. In such cases, not only are baseline shifts in the strong-motion accurately corrected, but also the high resolution acceleration records help to constrain the GPS for a better solution. As the two phases Kalman filter adaptively adjusted the estimation strategy, thus, more robust solutions can be provided.

Acknowledgments

We thank our colleagues for their technical supports in the experiment and Dr. Maorong Ge for his meaningful discussion. The K-Net strong-motion data for the 2011 Tohoku earthquake were provided by the National Research Institute for Earth Science and Disaster Prevention (NEID) of Japan. The GPS data were provided by the Geospatial Information Authority (GSI). Mr. Rui Tu is supported by China Scholarship Council for his Ph.D. study in Germany. In addition, the comments of the editor and two anonymous reviewers were very helpful for improving the quality and readability of the paper.

References

Bock, Y., Melgar, D., Crowell, B.W., 2011. Real-time strong-motion broadband displacements from collocated GPS and accelerometers. Bull. Seismol. Soc. Am. 101, 2904–2925.

Boore, D.M., 2001. Effect of baseline corrections on displacement and response spectra for several recordings of the 1999 Chi-Chi, Taiwan, earthquake. Bull. Seismol. Soc. Am. 91, 1199–1211.

Boore, D.M., Stephens, C.D., Joyner, W.B., 2002. Comments on baseline correction of digital strong-motion data: examples from the 1999 Hector Mine, California, earthquake. Bull. Seismol. Soc. Am. 92, 1543–1560.

Chiu, H., 1997. Stable baseline correction of digital strong-motion data. Bull. Seismol. Soc. Am. 87, 932–944.

Dach, R., Hugentobler, U., Fridez, P., Meindl, M. (Eds.), 2007. Bernese GPS software version 5.0. Astronomical Institute, University of Bern.

Elósegui, P., Davis, J.L., Oberlander, D., Baena, R., Ekström, G., 2006. Accuracy of high-rate GPS for seismology. Geophys. Res. Lett. 33, L11308. http://dx.doi.org/10.1029/2006GL026065.

Geng, J., Bock, Y., Melgar, D., Crowell, B.W., Haase, J.S., 2013a. A new seismogeodetic approach applied to GPS and accelerometer observations of the 2012 Brawley seismic swarm: implications for earthquake early warning. Geochem. Geophys. Geosyst. 14, 1–19. http://dx.doi.org/10.1002/ggge.20144.

Geng, J., Melgar, D., Bock, Y., Pantoli, E., Restrepo, L., 2013b. Recovering coseismic point ground tilts from collocated high-rate GPS and accelerometers. Geophys. Res. Lett. 40, 5095–5100. http://dx.doi.org/10.1002/grl.51001.

Genrich, J.F., Bock, Y., 2006. Instantaneous geodetic positioning with 10–50 Hz GPS measurements: noise characteristics and implications for monitoring networks. J. Geophys. Res. 111, B03403. http://dx.doi.org/10.1029/2005JB003617.

Graizer, V.M., 1979. Determination of the true ground displacement by using strong motion records. Izv. Earth Phys. 15, 875–885.

Graizer, V.M., 2005. Effect of tilt on strong motion data processing. Soil Dyn. Earthquake Eng. 25, 197–204.

Graizer, V.M., 2006. Tilts in strong ground motion. Bull. Seismol. Soc. Am. 96, 2090–2106.

Hauschild, A., Montenbruck, O., 2009. Kalman-filter-based GPS clock estimation for near real-time positioning. GPS Solut. 13 (3), 173–182.

Hu, C.W., Chen, W., Chen, Y.Q., Liu, D.J., 2003. Adaptive Kalman filtering for vehicle navigation. J. Global Positioning Syst. 2 (1), 42–47.

Huang, J., Wen, K., Li, X., Xie, J., Chen, C., Su, S., 2013. Coseismic deformation time history calculated from acceleration records using an EMD-Derived baseline correction scheme: a new approach validated for the 2011 Tohoku earthquake. Bull. Seismol. Soc. Am. 103, 1321–1335.

Iwan, W., Moser, M., Peng, C., 1985. Some observations on strong-motion earthquake measurement using a digital accelerograph. Bull. Seismol. Soc. Am. 75, 1225–1246.

Jin, S.G., Wang, J., Park, P.H., 2005. An improvement of GPS height estimations: stochastic modeling. Earth Planets Space 57 (4), 253–259.

Jin, S.G., Luo, O.F., Ren, C., 2010. Effects of physical correlations on long-distance GPS positioning and zenith tropospheric delay estimates. Adv. Space Res. 46 (2), 190–195. http://dx.doi.org/10.1016/j.asr.2010.01.017.

Kouba, J., Héroux, P., 2001. Precise point positioning using IGS orbit and clock products. GPS Solut. 5 (2), 12–28. http://dx.doi.org/10.1007/PL00012883.

Larson, K.M., Bilich, A., Axelrad, P., 2007. Improving the precision of high-rate GPS. J. Geophys. Res. 112, B05422. http://dx.doi.org/10.1029/2006JB004367.

Tu, R., Wang, R., Ge, M., Walter, T.R., Ramatschi, M., Milkereit, C., Bindi, D., Dahm, T., 2013. Cost-effective monitoring of broadband strong ground motion related to earthquakes, landslides or volcanic activities by joint use of a single-frequency GPS and a MEMS-type accelerometer. Geophys. Res. Lett. 40, 3825–3829. http://dx.doi.org/10.1002/grl.50653.

Tu, R., Ge, M., Wang, R., Walter, T.R., 2014. A new algorithm for tight integration of real-time GPS and strong-motion records, demonstrated on simulated, experimental, and real seismic data. J. Seismol. 18, 151–161. http://dx.doi.org/10.1007/s10950-013-9408-x.

Walter, T.R., 2011. Low cost volcano deformation monitoring: optical strain measurements and application to Mount St. Helens data. Geophys. J. Int. 186 (2), 699–705. http://dx.doi.org/10.1111/j.1365'-246X.2011.05051.x.

Wang, J., Stewart, M.P., Tsakiri, M., 2000. Adaptive Kalman filtering for integration of GPS with GLONASS and INS. Int. Assoc. Geod. Symp. 121, 325–330.

Wang, R., Schurr, B., Milkereit, C., Shao, Z., Jin, M., 2011. An improved automatic scheme for empirical baseline correction of digital strong-motion records. Bull. Seismol. Soc. Am. 101, 2029–2044.

Wang, R., Parolai, S., Ge, M., Jin, M., Walter, T., Zschau, J., 2013. The 2011 Mw 9.0 Tohoku earthquake: comparison of GPS and strong-motion data. Bull. Seismol. Soc. Am. 103, 1336–1347. http://dx.doi.org/10.1785/0120110264.

Wu, Y., Wu, C., 2007. Approximate recovery of coseismic deformation from Taiwan strong-motion records. J. Seismol. 11, 159–170.

Yang, Y., Gao, W., 2006. A new learning statistic for adaptive filter based on predicted residuals. Prog. Nat. Sci. 16 (8), 833–837.

Yang, Y., He, H., Xu, G., 2001. Adaptively robust filtering for kinematic geodetic positioning. J. Geodesy. 75, 109–116.

Zhu, L., 2003. Recovering permanent displacements from seismic records of the June 9, 1994 Bolivia deep earthquake. Geophys. Res. Lett. 30, 1740. http://dx.doi.org/10.1029/2003GL017302.

Please cite this article in press as: Tu, R., et al. Adaptive recognition and correction of baseline shifts from collocated GPS and accelerometer using two phases Kalman filter. J. Adv. Space Res. (2014), http://dx.doi.org/10.1016/j.asr.2014.07.008